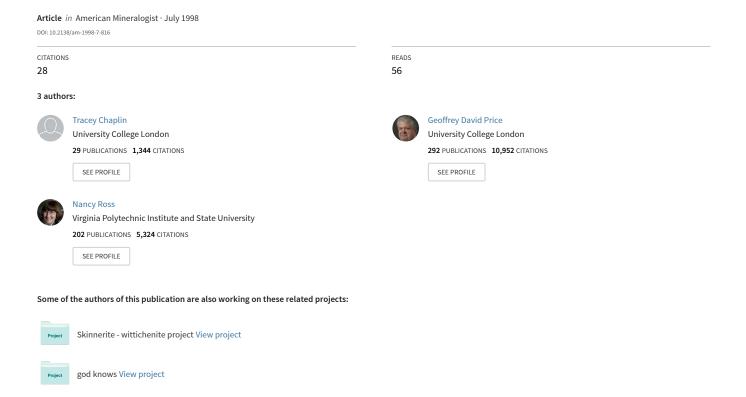
# Computer simulation of the infrared and Raman activity of pyrope garnet, and assignment of calculated modes to specific atomic motions



## Computer simulation of the infrared and Raman activity of pyrope garnet, and assignment of calculated modes to specific atomic motions

TRACEY CHAPLIN,\* G. DAVID PRICE, AND NANCY L. ROSS

Research School of Geological and Geophysical Sciences, University College London, Gower Street, London WC1E 6BT, U.K.

#### **ABSTRACT**

The lattice dynamics computer code PARAPOCS was successfully used to calculate the 240 vibrational frequencies of pyrope garnet, Mg<sub>3</sub>Al<sub>2</sub>Si<sub>3</sub>O<sub>12</sub>, at ambient conditions. The atomic displacement vectors (eigenvectors) for each frequency were also calculated and their symmetry relations analyzed with the aid of factor group analysis (FGA), to determine the symmetry species of each vibrational mode. Comparison with the experimental IR and Raman data shows excellent agreement, but no LO-TO reversals were identified. Calculation of the frequency shifts due to the isotopic substitution of <sup>26</sup>Mg and <sup>30</sup>Si, together with a more detailed analysis of the calculated eigenvectors, enabled identification of the dominant site or cation motion contributing to each vibrational mode. Previous assignments of the high-frequency vibrations to pure SiO<sub>4</sub> internal modes and the lower-frequency vibrations to mixed cation modes are supported. We conclude that the specific number of site/atom motions predicted by site group analysis (SGA) is not adhered to due to substantial mode mixing, and that FGA and SGA, in which the SiO<sub>4</sub> tetrahedra are treated as isolated units, are only applicable at high frequencies. The agreement observed between the calculated and experimental data leads us to conclude that the method of computer modeling used and the interatomic potentials employed in the simulations provide a good description of the lattice dynamical behavior of pyrope garnet.

#### Introduction

Garnets are important metamorphic minerals observed at the Earth's surface and are fundamental constituents of the Earth's upper mantle and transition zone. According to most petrological models, the garnet solid-solution series forms approximately 15% of the upper mantle and this volume fraction increases in the transition zone due to the dissolution of up to 80% pyroxene into the garnet structure (Ringwood 1967, 1970; Akaogi and Akimoto 1977; Gasparik 1989). Below 300 km, pyrope, Mg<sub>3</sub>-Al<sub>2</sub>Si<sub>3</sub>O<sub>12</sub>, forms an important solid-solution with majorite, Mg<sub>4</sub>Si<sub>4</sub>O<sub>12</sub> (Ringwood and Major 1971; Akaogi and Akimoto 1977; McMillan et al. 1989; Gasparik 1989, 1990; Sinogeiken et al. 1997; Heinemann et al. 1997). Hence, it is important to have an accurate determination of the vibrational properties of pyrope as these govern its macroscopic behavior and therefore influence the characteristics of the phases along the binary join.

Powder-dispersion IR spectra of pyrope-rich garnets (Adler et al. 1950; Launer 1952; Wickersheim et al. 1960; Tarte 1965; Moore et al. 1971; Cahay et al. 1981; Geiger et al. 1989, 1992; and Bosenick et al. 1995) commonly yield fewer than the expected 17 modes. Measurements of this type encounter significant scattering and give peak positions that lie between the LO and TO frequencies according to the powder density and particle thickness

used. In contrast, the single-crystal reflectance data of Hofmeister and Chopelas (1991) and Hofmeister et al. (1996) give a quantitative and complete set of IR-active bands for pyrope and demonstrate that accidental degeneracies occur for two of the IR modes.

Raman spectroscopic studies of pyrope-rich garnets are less common. Griffith (1969) presented six Raman-active bands in the range 300–1000 cm<sup>-1</sup>, and the subsequent Raman studies were still limited when Mernagh and Liu (1990) reported only 7 out of the expected 25 Raman-active modes in the range 100–1200 cm<sup>-1</sup>. Hofmeister and Chopelas (1991) made polarized single-crystal Raman measurements of pyrope and reported the first complete set of 25 Raman-active bands. Later studies by authors such as Kolesov and Geiger (1998) and Gillet et al. (1992) have presented a maximum of 17 and 19 bands, respectively, in the same range.

The number of IR and Raman spectroscopic studies of garnets with various compositions reporting incomplete sets of modes illustrates the necessity for single-crystal and polarized studies of solid-solutions, and the care required to distinguish between weak modes and artifacts. Computer simulations can augment these difficult experiments through the prediction of vibrational frequencies and their IR and Raman-activity. In this paper, we present the first complete set of calculated Raman-active and IRactive vibrational modes (including LO-TO splittings) for pyrope garnet. We also assign the modes to dominant site

<sup>\*</sup> E-mail: t.chaplin@ucl.ac.uk

or cation motions, determined from the calculated atomic displacements and calculated mode shifts due to the isotopic substitution of <sup>26</sup>Mg and <sup>30</sup>Si.

#### COMPUTATIONAL METHOD

Garnets have a cubic structure (space group  $Ia\overline{3}d$ ), with formula X<sub>3</sub>Y<sub>2</sub>Si<sub>3</sub>O<sub>12</sub>, and may be described in terms of independent SiO<sub>4</sub> tetrahedra linked to YO<sub>6</sub> octahedra by corner sharing  $(Y = Al, Fe^{3+}, Cr)$ . These polyhedra form the basic three-dimensional framework of the structure, with intervening triangular-dodecahedral sites containing the X (Mg, Fe, Ca, Mn) divalent cations (Novak and Gibbs 1971). Menzer (1926) established that the X cations have  $D_2$  site symmetry, the Y cations  $S_6$  symmetry, the Si cations S<sub>4</sub> symmetry, with the O atoms in general sites C<sub>1</sub>. The smallest Bravais cell is primitive with four formula units or 80 atoms per unit cell. As there are 3n degrees of vibrational freedom in a structure, there will be 240 degrees of vibrational freedom in the primitive unit cell of garnet. These modes were calculated using the lattice dynamics computer code PARAPOCS (Parker and Price 1989). This program is based on the classical Born approach to modeling solids (Born and Huang 1954) in which interatomic potentials are used to define the net forces acting between the atoms in the structure. The short-range repulsive and attractive dispersive forces were modeled in this study using Buckingham potentials for each pairwise interaction, with a shell model used to describe the ionic polarizability of the O atoms. The directionality of the O-Si-O bond was modeled by introducing a three-body term into the potential, as used by Sanders et al. (1984). Our simulations employed the potential parameters defined by Lewis and Catlow (1985) and Sanders et al. (1984) for simple oxides, which previously have been shown to give a good description of the structural, elastic, and thermodynamic properties of pyrope and other silicate minerals (e.g., Patel et al. 1991; Price et al. 1987), without optimization to fit experimental

The relationship between the interatomic potential and the normal vibrational modes of a solid have been described in detail by authors such as Born and Huang (1954), Ziman (1964), and Cochran (1973). A brief description of the derivation of the 3n sets of eigenvectors  $[(\mathbf{e}_{\mathbf{x}}(\mathbf{q}), \mathbf{e}_{\mathbf{y}}(\mathbf{q}), \mathbf{e}_{\mathbf{z}}(\mathbf{q})]$ , which describe the Cartesian components of the atomic displacements for each normal mode  $\mathbf{q}$ , may be found in Patel et al. (1991) and Price et al. (1987).

Thus, we have used the computer code PARAPOCS to calculate the 240 vibrational frequencies of the primitive unit cell of pyrope, together with their associated eigenvectors (using the fractional coordinates from the relaxed structure), under ambient conditions at a point close to the Brillouin zone center. Calculations of this type cannot be made at precisely the zone center, where the acoustic modes are zero, and so our simulations were performed at  $\mathbf{k} = (0.0, 0.0, 0.0001)$ . Calculation of the longitudinal acoustic mode as  $0.06 \text{ cm}^{-1}$  at this point suggests that this

is the error in the calculated frequencies of the optic modes.

The highly symmetric garnet structure contains 48 symmetry elements and belongs to the  $O_h$  point group. Factor group analysis (FGA) of the garnet structure (e.g., Moore et al. 1971; Fateley et al. 1972) predicts the following symmetry for the vibrational modes:

$$\Gamma_{\text{total}} = 3A_{1g} + 5A_{2g} + 8E_g + 14F_{1g} + 14F_{2g} + 5A_{1u}$$

$$+ 5A_{2u} + 10E_u + 18F_{1u} + 16F_{2u}$$
(1)

A total of 17 infrared-active  $(17F_{1u})$  and 25 Ramanactive  $(3A_{1g} + 8E_g + 14F_{2g})$  modes are therefore expected. The 125 remaining modes are optically inactive; it may also be seen that one additional  $F_{1u}$  mode is acoustic in character. Site group analysis (SGA) of the garnet structure (Moore et al. 1971; Fateley et al. 1972) illustrates the relationship between these symmetry species and cation site motion. The eigenvectors calculated for each vibrational frequency were analyzed to ascertain which symmetry elements were maintained after the displacements of the atoms. This procedure allows identification of the symmetry species for each vibrational mode and hence, determination of their Raman- or IR-activity. This was achieved using the  $O_h$  point group character table (e.g., Fateley et al. 1972), in which the positive values contained in the table indicate those symmetry elements that are maintained during a vibration associated with a particular symmetry species. Similarly, the negative values in the table show which symmetry elements must be destroyed in order for a vibration to belong to a particular symmetry species.

The vibrational frequencies of pyrope were also calculated using isotopic substitution of <sup>26</sup>Mg and <sup>30</sup>Si into the pyrope structure. Analysis of the mode shifts arising from these substitutions, together with further analysis of the calculated eigenvectors, enabled the dominant site or cation motion contributing to each vibrational mode to be identified.

### COMPARISON OF CALCULATED AND EXPERIMENTAL VIBRATIONAL FREQUENCIES

#### **Infrared-active modes**

The calculated infrared-active modes of pyrope are presented in Table 1 together with the observed modes from the most comprehensive experimental IR study (Hofmeister et al. 1996) for comparison. The calculated IR modes are characterized by three components: (1) a single longitudinal optic (LO) mode (2) associated with a doubly degenerate transverse optic (TO) mode that (3) is always lower in frequency than the LO mode. The LO mode associated with each TO pair is easily identifiable from our analysis of the eigenvectors calculated for each frequency. The column sum of the eigenvector matrix for each atom species gives values x, y, and z for the first TO component and -y, x, z for the second TO component, where z is always zero. The corresponding LO component has eigenvector matrix column totals z, z, |y-x|,

as required by the propagation directions of the LO and TO wave components. This analysis has resulted in the pairings of the calculated LO and TO modes shown in Table 1 and consequently no LO-TO reversals, in which the TO component of an LO-TO pair is higher in frequency than its associated LO mode, were identified. Such reversals have been documented in quartz (Scott and Porto 1967) and garnet (Hofmeister and Chopelas 1991; Hofmeister et al. 1996) when a low-intensity band occurs just above and very close to a band of high intensity, resulting in the TO frequency of the weaker band being greater than its corresponding LO component. Although four such reversals were reported by Hofmeister and Chopelas (1991) for LO-TO pairs at 889-906, 528-536, 474–478, and 422–423 cm<sup>-1</sup>, this number was reduced to two by Hofmeister et al. (1996) for the peaks at 902-890 and 478-475 cm<sup>-1</sup>. Recently however, this has been reduced to a single reversal at 475–478 cm<sup>-1</sup> (A. Hofmeister, personal communication). The calculated eigenvectors unambiguously show that no reversals are present in the calculated modes and we therefore do not support the observation that LO-TO reversals occur in pyrope.

Our simulated IR modes show excellent agreement with those calculated by Winkler et al. (1991) using a lattice dynamical model, with an average difference of approximately 7 cm<sup>-1</sup>. Table 1 shows that there is also generally very good agreement between the calculated  $F_{1u}$  frequencies and those reported by Hofmeister et al. (1996). For example, the calculated LO-TO pairs at 1068.1–973.8 cm<sup>-1</sup> and 402.5–380.7 cm<sup>-1</sup> differ only slightly from the observed pairings at 1060–972 cm<sup>-1</sup> and 400–383 cm<sup>-1</sup>, respectively.

Our calculated LO-TO pair at 709.6–681.4 cm<sup>-1</sup> shows poor agreement with the mode at 650 cm<sup>-1</sup> reported by Hofmeister et al. (1996). This may be because the position of this observed mode is approximate, and a better comparison may be made with the LO-TO pair reported at 667–664 cm<sup>-1</sup> (Hofmeister and Chopelas 1991). The calculated LO-TO pair at 442.9–432.1 cm<sup>-1</sup> has no comparable observed value in the reflectance data sets of Hofmeister et al. (1996) or Hofmeister and Chopelas (1991). An  $F_{1u}$  mode of similar energy (450 cm<sup>-1</sup>) was reported in the data set of Winkler et al. (1991), and the small calculated LO-TO splitting for this mode suggests that it may be more favorably compared with the bands at approximately 455 cm<sup>-1</sup> reported by Moore et al. (1971) for powder data on pyrope-rich samples.

The observed mode reported by Hofmeister et al. (1996) at 357–336 cm<sup>-1</sup> shows poor agreement with our calculated LO-TO pair at 318.8–316.9 cm<sup>-1</sup>; the calculated pair at 273.4–273.3 cm<sup>-1</sup> also has no experimental equivalent. This may be related to the accidental degeneracy reported by Hofmeister et al. (1996) for this mode from their observation that two pairs of peaks (336 and 134 cm<sup>-1</sup>) coalesced in the very pyrope-rich spectrum of the pyrope-almandine solid-solution. However, the calculated mode at 273.4–273.3 cm<sup>-1</sup> is highly comparable

**TABLE 1.** Observed (Hofmeister et al. 1996) and calculated infrared-active modes of pyrope, and their mode assignments (units = cm<sup>-1</sup>)

	Observed mod	des	Calculated modes			
Assign- ment	LO modes	TO modes	LO modes	TO modes	Assign- ment	
ν <sub>3</sub> ν <sub>3</sub> ν <sub>3</sub> ν <sub>4</sub> ν <sub>4</sub> ν <sub>4</sub> ν <sub>4</sub> ν <sub>4</sub>	1060 941 890 ~650 620 557 530 475	972 902* 871* ~650 581 535 455 478	1068.1 913.4 877.4 709.6 636.5 610.5 532.3 486.3 442.9	973.8 878.3 841.2 681.4 610.6 556.1 493.8 475.5 432.1	ν <sub>3</sub> ν <sub>3</sub> ν <sub>4</sub> ν <sub>4</sub> ν <sub>4</sub> ν <sub>2</sub> Τ(Al) Τ(Al)	
T(AI)	423	422	431.5	417.1	T(Mg) R(SiO₄) T(Mg)	
$R(SiO_4)$ $R(SiO_4)$ $T(SiO_4)$	400 357† 357†	383 336 336	402.5 318.8	380.7 316.9	T(AI) T(Mg) T(SiO <sub>4</sub> ) R(SiO <sub>4</sub> )	
T(AI) T(Mg)	263 223	259 221	273.4 257.4 231.0	273.3 234.6 230.9	T(Mg) T(Mg) T(SiO₄) T(Mg)	
T(Mg) T(Mg) T(SiO₄)	218 152† 152†	195 134 134	172.8 156.0	170.4 153.1	T(Mg) T(SiO₄) T(Mg)	

<sup>\*</sup> Previous LO and TO reversal was eliminated as this assignment was equivocal (A. Hofmeister, personal communication).

with the mode reported at approximately 272 cm<sup>-1</sup> by Hofmeister and Chopelas (1991), and the very small LO-TO splitting of the calculated mode at 318.8–316.9 cm<sup>-1</sup> suggests that it may be more favorably compared with the powder spectra reported by Moore et al. (1971) in the range 308–325 cm<sup>-1</sup> for pyralspite garnets.

#### Raman-active modes

The calculated Raman-active modes of pyrope are presented in Table 2, together with the modes determined by Kolesov and Geiger (1998) and Hofmeister and Chopelas (1991) from their fully polarized single-crystal studies. The calculated Raman modes may be grouped into three distinct regions: low frequency peaks (192–431 cm<sup>-1</sup>); medium energy peaks (473–644 cm<sup>-1</sup>); and high energy peaks (815–1062 cm<sup>-1</sup>), with one  $A_{1g}$  peak located in each region. These groupings show excellent agreement with those made by Hofmeister and Chopelas (1991).

The calculated  $A_{1g}$  modes show reasonable agreement with the  $A_{1g}$  modes reported by Kolesov and Geiger (1998) and Hofmeister and Chopelas (1991), with the calculated modes lower in frequency than the observed bands. The agreement between the data sets was observed to improve at the lower frequencies. The discrepancies between the observed and calculated data may be related to the Si-O potential or the three-body bending term employed in the model, which may not fully describe the behavior of the SiO<sub>4</sub> tetrahedra in this case.

Comparison of the calculated  $E_g$  modes with the ob-

<sup>†</sup> Degeneracies determined from the solid-solution of pyrope and almandine.

**TABLE 2.** Observed and calculated Raman-active modes of pyrope (units =  $cm^{-1}$ )

Symmetry		Observed modes and assignments				Calculated modes and assignments		
species	Assignment*	Mode*	Assignment†	Mode†	Mode‡	Assignment‡		
$\overline{A_{1g}}$	(Si-O) <sub>str</sub>	928	$\nu_1$	925	850.5	$\nu_1$		
$A_{1g}$	(Si-O) <sub>bend</sub>	563	$\nu_2$	562	524.0	$\nu_{2}$		
$A_{1g}$	R(SiO <sub>4</sub> )	364	R(SiO <sub>4</sub> )	362	342.7	R(SiO <sub>4</sub> )		
E <sub>a</sub>	(Si-O) <sub>str</sub>	945	$\nu_3$	938	943.1	$\nu_3$		
$E_g$ $E_g$ $E_g$ $E_g$ $E_g$ $E_g$ $E_g$		_	$\nu_1$	911(867§)	816.3	$\nu_1$		
Ĕ <sub>a</sub>	_	_	$\nu_4$	626	633.2	$\nu_4$		
E <sub>a</sub>	(Si-O) <sub>bend</sub>	525	$\nu_2$	524	506.8	$\nu_2$		
E <sub>a</sub>	_	_	$\nu_2$	439	430.6	$\nu_2$		
Ĕ.	(Si-O) <sub>bend</sub>	375	R(SiO <sub>4</sub> )	365(379§)	363.8	R(SiO <sub>4</sub> )		
E <sup>°</sup>	R(SiO <sub>4</sub> )	344	T(SiO <sub>4</sub> )	342(309§)	307.7	R(SiO₄)		
g	T(Mg)	284	( 4)	(**************************************		T(Mg)		
$E_g$	T(SiO₄)	211	T(Mg)	203	207.2	T(SiO₄)		
— <i>g</i>	(-1-4)		(11.9)			T(Mg)		
$F_{2g}$	(Si-O) <sub>str</sub>	1066	$\nu_3$	1062	1061.8	$\nu_3$		
F <sub>2</sub> ,	(Si-O) <sub>str</sub>	902	$\nu_3$	899	875.8	$\nu_3$		
F-	(Si-O) <sub>str</sub>	871	$\nu_3$	866	844.4	$\nu_3$		
$F_{2g}^{2g}$ $F_{2g}$ $F_{2g}$	(Si-O) <sub>bend</sub>	650	$\nu_4$	648	643.8	$v_4$		
F-	(Si-O) <sub>bend</sub>	598	$v_4$	598	607.2	$v_4$		
$F_{2g} \ F_{2g} \ F$	(Si-O) <sub>bend</sub>	512	$v_4$	510	514.9	$v_4$		
F. 2g	(Si-O) <sub>bend</sub>	492	$v_2$	490	473.2	$v_2$		
F. 2g	R(SiO₄)	383	R(SiO₄)	379	367.3	R(SiO₄)		
F 2g	R(SiO₄)	353	R(SiO₄)	350	353.1	R(SiO <sub>4</sub> )		
<sup>1</sup> 2g	11(0104)	000	11(0104)	330	000.1	T(Mg)		
$F_{2g}$	R(SiO₄)	322	T(SiO <sub>4</sub> )	318(342§)	323.1	T(SiO <sub>4</sub> )		
* 2g	11(0104)	022	1 (3134)	010(0123)	020.1	?R(SiO <sub>4</sub> )		
$F_{2g}$	_	_	T(SiO <sub>4</sub> ) <sub>mix</sub>	285(318§)	297.2	T(Mg)		
· 2g			- ( 34/mix	===(3:03)		T(SiO <sub>4</sub> )		
$F_{2g}$	_	_	T(Mg)	272	246.6	T(Mg)		
· 2g			. (9)		210.0	T(SiO₄)		
$F_{2g}$	_	_	T(SiO <sub>4</sub> ) <sub>mix</sub>	230	227.4	T(Mg)		
$F_{2g}$	T(SiO <sub>4</sub> )	222	T(Mg)	208	192.6	T(Mg)		
' 2g	T(Mg)	135	1 (1419)	200	102.0	i (ivig)		

<sup>\*</sup> Kolesov and Geiger (1998).

served modes listed in Table 2 shows that there is excellent agreement between the data sets, with an average difference of approximately 7 cm<sup>-1</sup>, except for the calculated modes at 307 and 816 cm<sup>-1</sup>, which show greater deviations from the observed modes. However, the corresponding observed Raman modes at 911 and 342 cm<sup>-1</sup> recently have been revised to 867 and 309 cm<sup>-1</sup>, respectively (A. Chopelas et al., in preparation), which greatly improves the agreement with the calculated data.

The calculated  $F_{2g}$  modes show very good agreement with the observed modes listed in Table 2, with an average difference of 10 cm<sup>-1</sup> between the data sets. Kolesov and Geiger (1998) reported a low energy Raman mode at 135 cm<sup>-1</sup> in their  $F_{2g}$  spectrum, which was not reported by previous authors. It was attributed to the anisotropic dynamic disorder within the dodecahedral site, which causes the Mg-cation to undergo a "rattling" motion in the site (Armbruster et al. 1992). We did not observe this mode in our simulations, and this may be due to our use of the quasi-harmonic approximation, which does not include anharmonic effects. However, this mode may be related to the lowest-energy IR mode observed at 134 cm<sup>-1</sup> (Hofmeister et al. 1996) leaking through

into the Raman spectrum (A. Hofmeister, personal communication).

#### Mode assignments

The results of lattice dynamical simulations of the vibrational frequencies of pyrope with isotopic substitution of 30Si and 26Mg are shown in Tables 3-4. Analysis of the frequency shifts caused by the substitutions, together with a more detailed analysis of the calculated eigenvectors, allowed the dominant site or cation motion contributing to each vibrational mode to be determined (Tables 1-2). SGA (e.g., Moore et al. 1971) provides the expected number of site or atomic motions for each symmetry species. However, assignment of the calculated modes shows that the atomic motions predicted by SGA are not always adhered to. The high-frequency vibrations were observed to comply strictly with the SiO<sub>4</sub> internal modes predicted by SGA. However, at lower frequencies (<450 cm<sup>-1</sup>), mixing of modes was observed to occur, in which more than one specific site or cation motion contributes to a vibration.

<sup>†</sup> Hofmeister and Chopelas (1991).

<sup>‡</sup> This study.

<sup>§</sup> Revisions in frequency (Chopelas et al., in preparation).

Table 3. Effect of <sup>30</sup>Si and <sup>26</sup>Mg substitution on calculated IRactive (TO) modes

Mg <sub>3</sub> Al <sub>2</sub> Si <sub>3</sub> O <sub>12</sub>	Mg <sub>3</sub> Al <sub>2</sub> <sup>30</sup> Si <sub>3</sub> O <sub>12</sub>			<sup>26</sup> Mg <sub>3</sub> Al <sub>2</sub> Si <sub>3</sub> O <sub>12</sub>		
ν (cm <sup>-1</sup> )	$\nu$ (cm <sup>-1</sup> )	$\frac{\Delta\nu}{(\text{cm}^{-1})}$	Δν (%)	ν (cm <sup>-1</sup> )	$\frac{\Delta\nu}{(\text{cm}^{-1})}$	Δν (%)
973.8 878.3 841.2 681.3 610.5 556.1 493.8 475.5 432.1 417.0 380.7 316.9 273.3	954.3 872.3 829.0 680.6 609.7 554.4 493.1 474.4 430.6 416.9 379.4 315.6 272.8	19.5 6.0 12.2 0.7 0.8 1.7 0.7 1.1 1.5 0.1 1.3 1.3	2.04 0.69 1.48 0.10 0.13 0.31 0.14 0.23 0.35 0.02 0.34 0.41	971.9 878.0 841.1 679.6 609.9 555.8 492.3 474.9 423.3 408.4 379.6 316.1 269.8	1.9 0.3 0.1 1.7 0.6 0.3 1.5 0.6 8.8 8.6 1.1 0.8 3.5	0.19 0.03 0.01 0.25 0.10 0.05 0.30 0.13 2.08 2.11 0.29 0.25 1.30
234.6 230.9 170.4 153.1	233.8 229.1 170.1 152.1	0.8 1.8 0.3 0.1	0.34 0.79 0.18 0.66	231.4 226.8 167.9 152.0	3.2 4.1 2.5 1.1	1.38 1.81 1.49 0.72

#### Infrared modes

The site group analysis of garnet predicts that of the IR-active modes there should be: 1  $\nu_2$  symmetric bending, 3  $\nu_3$  asymmetric stretching, and 3  $\nu_4$  asymmetric bending SiO<sub>4</sub> internal modes; 2 SiO<sub>4</sub>-rotational, R(SiO<sub>4</sub>), 3-1 SiO<sub>4</sub>-translational, T(SiO<sub>4</sub>), 3 Mg-translational, T(Mg), and 3 Al-translational, T(Al), modes. Analysis of the calculated frequency shifts with isotopic substitution, which show good agreement with those reported by Cahay et al. (1981), combined with further analysis of the calculated eigenvectors, has resulted in the assignments of the calculated IR-active modes shown in Table 1.

Our assignments of the high-frequency modes show that they all are attributable to the internal stretching and bending modes of the  $SiO_4$  tetrahedra, with greatest frequency shifts observed for the  $\nu_3$  modes. Comparison with the modes predicted by SGA and the assignments of Hofmeister et al. (1996), made by counting down from the highest energy fundamentals assuming the sequence  $\nu_3 > \nu_1 > \nu_4 > \nu_2$ , shows that there is excellent agreement between the expected number of each of the  $\nu_1 - \nu_4$  modes and our own assignments.

Assignment of the calculated modes to Al-cation translations, via eigenvector analysis, has positioned the first 2 T(Al) directly below the SiO<sub>4</sub> internal modes, in agreement with Hofmeister et al. (1996). However, we have assigned the calculated mode at 442.9–432.1 cm<sup>-1</sup>, which was not observed by Hofmeister et al. (1996), as the second T(Al). The assignment of the observed mode of Hofmeister et al. (1996) at 423–422 cm<sup>-1</sup> as the second T(Al) therefore disagrees with our own. Analysis of the eigenvectors for the mode at 431.5–417.1 cm<sup>-1</sup>, considered to correspond to this observed mode, shows that it is dominated by SiO<sub>4</sub>-rotatory motions (with some Mg-cation movement) and that the Al cations have little involvement in this vibration. Our assignment of the final T(Al) to the mode at 402.5–380.7 cm<sup>-1</sup> differs significantly from that

**TABLE 4.** Effect of <sup>30</sup>Si and <sup>26</sup>Mg isotopic substitution on calculated Raman-active modes

N	Mg <sub>3</sub> Al <sub>2</sub> Si <sub>3</sub> O <sub>12</sub>	Mg <sub>3</sub> Al <sub>2</sub> <sup>30</sup> Si <sub>3</sub> O <sub>12</sub>			<sup>26</sup> Mg <sub>3</sub> Al <sub>2</sub> Si <sub>3</sub> O <sub>12</sub>		
	(ann -1)	(am=1)	Δν (am=1)	A - (0/)	(om-1)	Δν (am=1)	A - (0/)
_	ν (cm <sup>-1</sup> )	ν (cm <sup>-1</sup> )	(cm <sup>-1</sup> )	$\Delta \nu$ (%)	ν (cm <sup>-1</sup> )	(cm <sup>-1</sup> )	$\Delta \nu$ (%)
	1061.8	1044.0	17.8	1.70	1060.9	0.9	0.08
	943.1	925.1	18.0	1.95	941.5	1.6	0.17
	875.8	863.7	12.1	1.40	875.6	0.2	0.02
	850.5	850.5	0.0	0.00	850.5	0.0	0.00
	844.3	838.7	5.6	0.67	844.2	0.1	0.01
	816.3	816.2	0.1	0.01	816.3	0.0	0.00
	643.8	642.0	1.8	0.28	643.7	0.1	0.02
	633.2	631.5	1.7	0.27	630.7	2.5	0.40
	607.2	605.9	1.3	0.21	607.1	0.1	0.02
	524.0	524.0	0.0	0.00	524.0	0.0	0.00
	514.9	511.8	3.1	0.61	514.7	0.2	0.04
	506.8	506.5	0.3	0.06	506.8	0.0	0.00
	473.2	471.8	1.4	0.30	473.1	0.1	0.02
	430.6	429.4	1.2	0.28	421.1	9.5	2.26
	367.3	367.0	0.3	0.08	367.0	0.3	0.08
	363.8	363.4	0.4	0.11	363.2	0.6	0.17
	353.1	352.2	0.9	0.26	347.4	5.7	1.64
	342.7	342.7	0.0	0.00	342.7	0.0	0.00
	323.1	320.6	2.5	0.78	322.7	0.4	0.12
	307.7	307.7	0.0	0.00	304.4	3.3	1.08
	297.2	296.1	1.1	0.37	292.2	5.0	1.71
	246.6	246.0	0.6	0.24	242.9	3.7	1.52
	227.4	227.1	0.3	0.13	225.1	2.3	1.02
	207.2	205.3	1.9	0.93	205.2	2.0	0.97
	192.6	192.3	0.3	0.16	188.8	3.8	2.01

of Hofmeister et al. (1996), who designated their observed mode at 259 cm<sup>-1</sup> as dominated by the final T(Al) mode, based on compositional/TO positional trends in the IR spectra of pyrope-almandine garnets. Our calculations show substantial movement of the Al-cations (mixed with Mg-cation motions) during the vibration at 402 cm<sup>-1</sup>, indicating it to be the position of the final T(Al) mode. The eigenvectors for the calculated mode at 257.4–234.6 cm<sup>-1</sup> indicate only very slight movement of the Al cations during this vibration and that these motions are very small compared to their motions in the higher frequency levels; the isotopic substitution data show that this mode is in fact dominated by T(Mg). All data sets have, however, shown that T(Al) are present in pyrope at frequencies lower than 410 cm<sup>-1</sup>, which is considerably lower than the commonly assumed  $500-550\ cm^{-1}$ .

Comparison of the assignment of the vibrational modes to  $SiO_4$ -rotations shows that both this study and Hofmeister et al. (1996) have placed the rotations directly below the first two T(Al) modes. We determined two modes to be attributable to R(SiO<sub>4</sub>), as predicted by SGA. However, these modes are not pure but mixed with T(Mg) or T(SiO<sub>4</sub>) components. Hofmeister et al. (1996) assigned the mode at 357–336 cm<sup>-1</sup> as R(SiO<sub>4</sub>) mixed with T(SiO<sub>4</sub>) also, from the observed degeneracy, in agreement with our own assignment.

Assignment of the calculated modes to SiO<sub>4</sub>-translations demonstrated that no pure T(SiO<sub>4</sub>) modes could be identified, in agreement with the observations of Hofmeister et al. (1996). We identified three T(SiO<sub>4</sub>) modes from the calculated frequency shifts (as predicted by SGA), but again these were observed to be mixed with

either R(SiO<sub>4</sub>) or T(Mg). Assignment of the calculated modes to T(Mg) shows that three relatively pure modes could be identified. The assignment of the calculated mode at 172.8–170.4 cm<sup>-1</sup> to T(Mg) is in excellent agreement with that of Hofmeister et al. (1996), and the similar assignment of the calculated mode at 273.4–273.3 cm<sup>-1</sup>, which was not formally identified by Hofmeister et al. (1996), shows excellent agreement with the assignment of Hofmeister and Chopelas (1991). (Assignment of the mode at 257.4-234.6 cm<sup>-1</sup> already has been discussed). Hofmeister et al. (1996) reported that the mode at 221 cm<sup>-1</sup> showed two-mode behavior in pyrope-almandine solid-solutions, indicating that this mode cannot be mixed. However, the calculated frequency shifts for the mode at 231.0–230.9 cm<sup>-1</sup> clearly show that this mode is related to movements of both the Si and Mg cations. This may be due to kinematic coupling of the Si and Mg cation sites, whereby movement of one set of cations automatically influences another.

#### Raman modes

SGA predicts that for the three symmetry species of Raman-active modes for pyrope, the  $A_{1g}$  modes are attributable to 1  $v_1$ , 1  $v_2$ , and 1 R(SiO<sub>4</sub>); the  $E_g$  modes to 1  $v_1$ , 2  $v_2$ , 1  $v_3$ , 1  $v_4$ , 1 R(SiO<sub>4</sub>), 1 T(SiO<sub>4</sub>), and 1 T(Mg); and the  $F_{2g}$  modes to 1  $v_2$ , 3  $v_3$ , 3  $v_4$ , 2 R(SiO<sub>4</sub>), 3 T(SiO<sub>4</sub>), and 2 T(Mg). The assignments of our calculated modes, made by analysis of the calculated frequency shifts with isotopic substitution (Table 4), are shown in Table 2. Of the Raman studies of pyrope published, only Hofmeister and Chopelas (1991) and Kolesov and Geiger (1998) have presented a full assignment of the Raman-active modes (Table 2). The latter authors used  $^{26}$ Mg isotopic substitution data to assist in the assignment of their observed Raman modes.

Comparison of the assignment of our calculated  $A_{1g}$  modes (Table 2) with those of Hofmeister and Chopelas (1991), Kolesov and Geiger (1998), and those expected from SGA, shows that there is complete agreement between all  $A_{1g}$  assignments. The calculated frequency shifts for the  $A_{1g}$  modes due to the isotopic substitution of  $^{30}$ Si (Table 4), demonstrate that these vibrations originate from the movements of the O atoms relative to the Si atom and hence, there appears to be no frequency change due to replacement of the Si atom.

Comparison of the assignments of the calculated internal  $E_s$  modes (Table 2) shows that there is also excellent agreement with the assignments of the experimentally determined modes and those predicted by SGA. However, assignments of the external modes show some differences. Our assignment of the calculated mode at 363.8 cm<sup>-1</sup> to R(SiO<sub>4</sub>) is in agreement with that of Hofmeister and Chopelas (1991), and we would suggest that the mode reported by Kolesov and Geiger (1998) at 375 cm<sup>-1</sup> is also attributable to R(SiO<sub>4</sub>), as originally suggested by them. The calculated mode at 307.7 cm<sup>-1</sup> also assigned as R(SiO<sub>4</sub>) shows good agreement with the assignment of the corresponding mode by Kolesov and Geiger (1998).

However, this disagrees with the number of R(SiO<sub>4</sub>) predicted by SGA and the assignment made by Hofmeister and Chopelas (1991) to T(SiO<sub>4</sub>). Our calculated frequency shifts for <sup>30</sup>Si substitution, together with analysis of the calculated eigenvectors, show that there is little or no movement of the Si cations during this vibration, and hence we suggest that it is attributable to SiO<sub>4</sub>-rotatory motions. The <sup>26</sup>Mg substitution data also suggest that this mode may contain an Mg-translatory component. The lowest energy  $E_a$  mode has been also assigned as a mixed mode, consisting of both SiO<sub>4</sub>- and Mg-translatory motions, by analysis of the calculated frequency shifts due to both isotopic substitutions. Kolesov and Geiger (1998) also observed a similar shift of approximately 1% with Mg substitution, but assigned this mode as T(SiO<sub>4</sub>) as the mode was not pure. Our assignment of two  $E_g$  modes as containing T(Mg), again differs from the single T(Mg) vibration predicted by SGA.

Comparison of the assignment of the calculated  $F_{2e}$  internal modes with the observed modes (Table 2) shows that there is excellent agreement between the data sets and those predicted by SGA. Assignment of the  $F_{2g}$ modes to R(SiO<sub>4</sub>) shows that there is excellent agreement between all data sets for the two external modes of highest frequency (range 350–380 cm<sup>-1</sup>). However, our calculated frequency shifts suggest that the mode at 353.1 cm<sup>-1</sup> may also be partly attributable to T(Mg). Below 350 cm<sup>-1</sup>, assignment of the calculated and observed external modes again differs. Our calculations suggest that the mode at 323 cm<sup>-1</sup> is dominated by T(SiO<sub>4</sub>), with a resultant frequency shift of approximately 1% due to 30Si substitution. This agrees with the assignment made by Hofmeister and Chopelas (1991), but differs from that made by Kolesov and Geiger (1998), who assigned this mode as an SiO<sub>4</sub>-rotation. As the calculated frequency shift indicates that the mode is not pure T(SiO<sub>4</sub>), we also suggest that it may be associated with some SiO<sub>4</sub>-rotational motions, as there is little movement of the Mgcations at this energy level.

We have designated the remaining calculated  $F_{2g}$  modes in the range  $100-300~\rm cm^{-1}$  as dominated by relatively pure Mg-translations due to the large (1-2%) calculated frequency shifts associated with the  $^{26}$ Mg substitution. However, the calculated frequency shifts suggest that these modes may contain smaller components of  $T(\rm SiO_4)$ . This is in agreement with the assignments of Hofmeister and Chopelas (1991). Kolesov and Geiger (1998) reported a frequency shift of nearly 1% with  $^{26}$ Mg substitution for their observed mode at approximately  $222~\rm cm^{-1}$ , but assigned it as  $T(\rm SiO_4)$  because the mode was not pure  $T(\rm Mg)$ . However, our calculated frequency shift of 0.16% for this mode with  $^{30}$ Si substitution suggests that it is in fact dominated by Mg-cation motions and should be designated  $T(\rm Mg)$ .

Our assignment of the calculated vibrational modes shows that the number and type of SiO<sub>4</sub> internal modes predicted by SGA are consistently adhered to for all symmetry species. However, the calculated external modes

show substantial amounts of mode mixing below 450 cm<sup>-1</sup>, with mixing of T(SiO<sub>4</sub>) and T(Mg) dominating. From consideration of the garnet structure, this kinematic coupling is to be expected as the SiO<sub>4</sub>-tetrahedra share opposite edges with the Mg-cation sites, and any movement of the Si-O bonds affect the dodecahedral sites also. Our calculated eigenvectors and isotopic substitution data thus support the previous observations of mode mixing but give a more detailed account of which atoms are moving under each frequency and to what extent. Thus we conclude, as have previous authors, that the SGA model in which the SiO<sub>4</sub>-tetrahedral units are treated as isolated features, provides a good description of the internal modes of a crystalline solid at high energies, but tends to break down at lower energies where mixing of modes may occur.

#### ACKNOWLEDGMENTS

Tracey Chaplin thanks NERC for studentship no. GT4/94/213/G, and RAL for use of their supercomputing facilities. We thank John Brodholt and John Street for their invaluable help with computing problems and the reviewers whose comments improved the manuscript.

#### REFERENCES CITED

- Adler, H.H., Bray, E.E., Stevens, N.P., Hunt, J.M., Keller, W.D., Pickett, E.E., and Kerr, P.F. (1950) American petroleum institute project 49, preliminary report, 8, section I.
- Akaogi, M. and Akimoto, S. (1977) Pyroxene-garnet solid-solution Mg<sub>4</sub>Si<sub>4</sub>O<sub>12</sub>-Mg<sub>3</sub>Al<sub>2</sub>Si<sub>3</sub>O<sub>12</sub> and Fe<sub>4</sub>Si<sub>4</sub>O<sub>12</sub>-Fe<sub>3</sub>Al<sub>2</sub>Si<sub>3</sub>O<sub>12</sub> at high pressures and high temperatures. Physics of the Earth and Planetary Interiors, 15, 90–106.
- Armbruster, T., Geiger, C.A., and Lager, G.A. (1992) Single-crystal X-ray structure study of synthetic pyrope almandine garnets at 100 and 293 K. American Mineralogist, 77, 512–521.
- Born, M. and Huang, K. (1954) The dynamical theory of crystal lattices, 420 p. Clarendon Press, Oxford, U.K.
- Bosenick, A., Geiger, C.A., Schaller, T., and Sebald, A. (1995) A <sup>29</sup>Si MAS NMR and IR spectroscopic investigation of synthetic pyrope-grossular garnet solid solutions. American Mineralogist, 80, 691–704.
- Cahay, R., Tarte, P., and Fransolet, A-M. (1981) Interprétation du spectre infrarouge de variétés isotopiques de pyropes synthétiques. Bulletin Minéral, 104, 193–200.
- Cochran, W. (1973) The dynamics of atoms in crystals. Edward Arnold, London, U.K.
- Fateley, W.G., Dollish, F.R., McDevitt, N.T., and Bentley, F.F. (1972) Infrared and Raman selection rules for molecular and lattice vibrations: the correlation method, 222 p. Wiley-Interscience, New York.
- Gasparik, T. (1989) Transformation of enstatite-diopside-jadeite pyroxenes into garnet. Contributions to Mineralogy and Petrology, 102, 389–405.
   ———(1990) Phase relations in the transition zone. Journal of Geophysical Research, 95, 15751–15769.
- Geiger, C.A., Merwin, L., and Sebald, A. (1992) Structural investigation of pyrope garnet using temperature-dependent FTIR and <sup>29</sup>Si and <sup>27</sup>Al MAS NMR spectroscopy. American Mineralogist, 77, 713–717.
- Geiger, C.A., Winkler, B., and Langer, K. (1989) Infrared spectra of synthetic almandine-grossular and almandine-pyrope garnet solid solutions: evidence for equivalent site behaviour. Mineralogical Magazine, 53, 231–237.
- Gillet, P., Fiquet, G., Malèzieux, J-M., and Geiger, C.A. (1992) Highpressure and high temperature Raman spectroscopy of end-member garnets: pyrope, grossular and andradite. European Journal of Mineralogy, 4, 651–664.
- Griffith, W.P. (1969) Raman studies on rock-forming minerals. Part 1: orthosilicates and cyclosilicates. Journal of the Chemical Society, 1969, 1372–1377.

- Heinemann, S., Sharp, T.G., Seifert, F., and Rubie, D.C. (1997) The cubic-tetragonal phase transition in the system majorite (Mg<sub>3</sub>Si<sub>4</sub>O<sub>12</sub>)-pyrope (Mg<sub>3</sub>Al<sub>2</sub>Si<sub>3</sub>O<sub>12</sub>), and garnet symmetry in the earth's transition zone. Physics and Chemistry of Minerals, 24, 206–221.
- Hofmeister, A.M. and Chopelas, A. (1991) Vibrational spectroscopy of end-member silicate garnets. Physics and Chemistry of Minerals, 17, 503–526
- Hofmeister, A.M., Fagan, T.J., Campbell, K.M., and Schaal, R.B. (1996) Single-crystal IR spectroscopy of pyrope-almandine garnets with minor amounts of Mn and Ca. American Mineralogist, 81, 418–428.
- Kolesov, B.A. and Geiger, C.A. (1998) Raman spectra of silicate garnets. Physics and Chemistry of Minerals, 25(2), 142–151.
- Launer, P.J. (1952) Regularities in the infrared absorption spectra of silicate minerals. American Mineralogist, 37, 764–784.
- Lewis, G.V. and Catlow, C.R.A. (1985) Potential models for ionic oxides. Physical Chemistry: Solid State Physics, 18, 1149–1161.
- McMillan, P., Akaogi, M., Ohtani, E., Williams, Q., Nieman, R., and Sato, R. (1989) Cation disorder in garnets along the Mg<sub>3</sub>Al<sub>2</sub>Si<sub>3</sub>O<sub>12</sub>-Mg<sub>4</sub>Si<sub>4</sub>O<sub>12</sub> join: an infrared, Raman and NMR study. Physics and Chemistry of Minerals, 16, 428–435.
- Menzer, G. (1926) Die Kristallstruktur von Granat. Zeitschrift für Kristallographie, 63, 157–158.
- Mernagh, T.P. and Liu, L-G. (1990) Pressure dependence of Raman spectra from the garnet end-members pyrope, grossularite and almandite. Journal of Raman Spectroscopy, 21, 305–309.
- Moore, R.K., White, W.B., and Long, T.V. (1971) Vibrational spectra of the common silicates: I. The garnets. American Mineralogist, 56, 54–71
- Novak, G.A. and Gibbs, G.V. (1971) The crystal chemistry of the silicate garnets. American Mineralogist, 56, 791–825.
- Parker, S.C. and Price, G.D. (1989) Computer modelling of phase transitions in minerals. Advances in Solid State Chemistry, 1, 295–327.
- Patel, A., Price, G.D., and Mendelssohn, M. (1991) A computer simulation approach to modelling the structure, thermodynamics and oxygen isotope equilibria of silicates. Physics and Chemistry of Minerals, 17, 690– 699.
- Price, G.D., Parker, S.C., and Leslie, M. (1987) The lattice dynamics of forsterite. Mineralogical Magazine, 51, 157–170.
- Ringwood, A.E. (1967) The pyroxene-garnet transformation in the earth's mantle. Earth and Planetary Science Letters, 2, 255–263.
- Ringwood, A.E. and Major, A. (1971) Synthesis of majorite and other high pressure garnets and perovskites. Earth and Planetary Science Letters, 12, 411–418.
- Sanders, M.J., Leslie, M., and Catlow, C.R.A. (1984) Interatomic potentials for SiO<sub>2</sub>. Journal of the Chemical Society, Section D: Chemical Communications, 19, 1271–1273.
- Scott, J.F. and Porto, S.P.S. (1967) Longitudinal and transverse optical lattice vibrations in quartz. Physical Review, 161(3), 903–910.
- Sinogeikin, S.V., Bass, J.D., O'Neill, B., and Gasparik, T. (1997) Elasticity of tetragonal end-member majorite and solid solutions in the system Mg<sub>4</sub>Si<sub>4</sub>O<sub>12</sub>-Mg<sub>3</sub>Al<sub>2</sub>Si<sub>3</sub>O<sub>12</sub>. Physics and Chemistry of Minerals, 24, 115–121
- Tarte, P. (1965) Étude experimentale et interpretation du spectre infrarouge des silicates et des germanates. Application á des problems structuraux relatifs a l'état solide. Bulletin de la Classe des Sciences Memoires (Academie Royale de Belgique), 35, 103–119.
- Wickersheim, K.A., Lefever, R.A., and Hanking, B.M. (1960) Infrared absorption spectra of the silicate ion in the garnet structure. Journal of Chemical Physics, 22, 271–276.
- Winkler, B., Dove, M., and Leslie, M. (1991) Static lattice energy minimization and lattice dynamics calculations on aluminosilicate minerals. American Mineralogist, 76, 313–331.
- Ziman, J.M. (1964) Principles of the theory of solids, 360 p. Cambridge University Press, Cambridge, U.K.

Manuscript received June 30, 1997 Manuscript accepted March 4, 1998 Paper handled by Hans Keppler